

Study on Continuous Hydrolysis in a Microchannel Reactor for the Production of Titanium Dioxide by a Sulfuric Acid Process

Wenbo Chang, Jianli Chen, Jun Dou, Bin Wu, Yu Rong Zhang,* and Kui Chen*

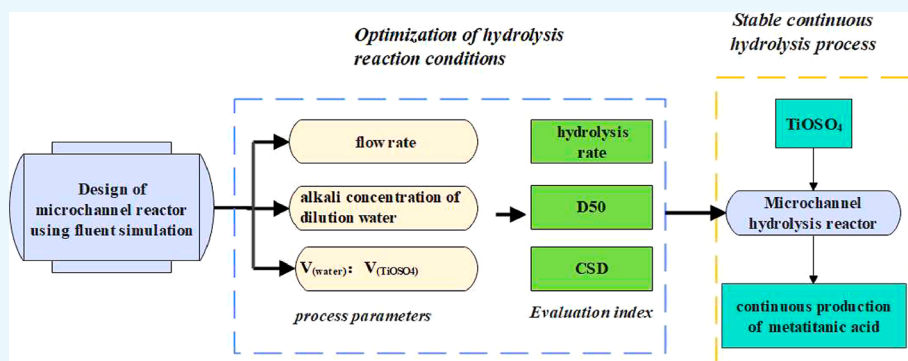
Cite This: *ACS Omega* 2022, 7, 22447–22455

Read Online

ACCESS |

Metrics & More

Article Recommendations



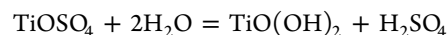
ABSTRACT: The development of a continuous hydrolysis process of titanium sulfate is an innovation to the traditional production process of titanium dioxide by the sulfuric acid process. In the experiment, a microchannel reactor was designed, and the hydrolysis rate of titanium sulfate, the particle size, and particle size distribution of metatitanic acid agglomerates were used as indicators to investigate the effect of operating conditions on the continuous hydrolysis of titanium sulfate. The results have shown that as the amount of dilution water increased, the hydrolysis rate of titanium sulfate decreased, and the particle size of primary aggregates of metatitanic acid increased from 39 to 54 nm. As the alkali mass concentration of dilution water increased, the hydrolysis rate of titanyl sulfate increased, and the particle size of primary aggregates of metastatic acid first decreased and then increased, and the particle size range was 40–48 nm. As the flow rate increased, the hydrolysis rate of titanyl sulfate increased, and the particle size of primary aggregates of metatitanic acid dropped from 59 to 43 nm. Compared with the batch hydrolysis operation, the continuous process has stronger anti-disturbance ability, significantly shorter operation time of the reaction section, and narrower particle size distribution of the product metatitanic acid.

1. INTRODUCTION

In China, more than 90% titanium dioxide (TiO_2) products are manufactured by a sulfate process. The hydrolysis process of titanyl sulfate (TiOSO_4) to produce amorphous metatitanic acid is an important step in the production of titanium dioxide by the sulfate process, which directly affects the hydrolysis rate of TiOSO_4 , the particle size, and particle size distribution of the hydrolysis product metatitanic acid. It also has an impact on the crystal form, particle size, and particle size distribution of the TiO_2 obtained by the subsequent calcination.¹ The hydrolysis of TiOSO_4 is an endothermic reaction process, accompanied by the emergence of gas and solid phases. The heat and mass transfer mechanisms of the reaction process are complicated, and the control of operating conditions is difficult. Limited by factors such as the temperature of the hydrolysis reaction ($>100\text{ }^\circ\text{C}$), corrosion of equipment materials, and equipment types, the hydrolysis process of TiOSO_4 has not yet achieved a continuous production process in industry. Discontinuous operation and lack of automatic

control cause the quality fluctuations of TiO_2 products. The quality of the sulfuric acid process TiO_2 product is lower than that of the chlorination process titanium dioxide product that uses continuous production, which limits the application of the sulfuric acid process TiO_2 in the high-end fields of downstream.^{2–5} Therefore, the development of a continuous hydrolysis process of titanyl sulfate is one of the effective ways to improve the quality of titanium dioxide.

The hydrolysis reaction of titanyl sulfate is as follows



Received: March 17, 2022

Accepted: June 7, 2022

Published: June 22, 2022



The reaction is an endothermic reaction, and the main factors affecting the conversion rate of TiOSO_4 are the total titanium concentration and the mass ratio of iron to titanium of the TiOSO_4 solution, the acidity value, and the reaction temperature.

Titanium ions exist in the form of Hexa-coordinated hydrated complex ions $[\text{Ti}(\text{H}_2\text{O})_6]^{4+}$ in the titanyl sulfate solution, and the coordinated water molecules can sometimes be replaced by other anions. The initial stage of hydrolysis titanyl sulfate proceeds with rapid breakup of chemical bonds,⁶ forming a colloidal complex. As the number of colloidal complexes increases, the rate of the hydrolysis reaction slows down. Santacesaria⁷ studied the hydrolysis kinetics of titanyl sulfate and established a mathematical model to explain the growth and particle size distribution of particles formed by hydrolysis. It was believed that the hydrolysis of the titanyl sulfate solution was the process of H^+ transfer and colloid aggregation. When the concentration of titanyl sulfate was high and the F value of titanyl sulfate solution was low, the aggregation of the colloid was dominant. When the F value of the titanyl sulfate solution was relatively high and the concentration of titanyl sulfate was low, the transfer reaction of H^+ was dominant. Tian,⁸ and Yu.⁹ both studied the effect of operating conditions on a batch hydrolysis process with autogenous seed crystals. It was found that various factors such as the F value, the amount of dilution water, heating rate, iron-titanium concentration ratio, and pH value of the dilution water affect the hydrolysis rate of titanyl sulfate, the nucleation rate of metatitanic acid, and the growth rate of titanium dioxide crystals in the subsequent calcination. Yang et al.¹⁰ found that reducing the heating rate of batch hydrolysis and adding an appropriate amount of low-concentration alkaline solution in the latter stage of the hydrolysis can make the particle size of the reaction product metatitanic acid more uniform, and the generation of small particles is effectively inhibited.

Sathyamoorthy et al.¹¹ studied the agglomeration mechanism of metatitanic acid during the hydrolysis process. The hydrolysis of titanyl sulfate to form metatitanic acid is a reactive crystallization process with added seed crystals, during which the formed metatitanic acid particles can be divided into three types according to their sizes—primary crystals (5–15 nm), primary agglomerated particles (30–80 nm), and secondary agglomerated particles (1–4 μm). Zhu et al.¹² pointed out that the crystal nuclei first formed primary crystals through crystal bridging, and then, several primary crystals agglomerated to form primary agglomerated particles. As the hydrolysis progressed, the primary agglomerated particles collided with each other and combined through the physical action of sulfate radicals to form secondary agglomerated particles, which was the form of the hydrolysis product metatitanic acid. The nucleation of metatitanic acid affected the structure and particle size of the agglomerates, and the effect of the number of seed crystals was significant. When a large amount of seed crystals was added, the supersaturation of the titanyl sulfate solution decreased rapidly, resulting in the formation of large-size primary agglomerates.

Some scholars conducted laboratory research on the continuous hydrolysis of titanyl sulfate in the kettle reactor. Grzmil¹³ found that the titanyl sulfate concentration and pH of titanyl sulfate had a significant influence on the hydrolysis rate when continuous hydrolysis reaction was carried out in one, two, and multiple reactors. In the multi-tank series reactor, the

feed rate and the residence time of the reaction solution were the main factors that affected the rate of hydrolysis. It is an effective way to increase the continuous hydrolysis rate of titanyl sulfate by using multiple tanks in series to reduce the concentration of free sulfuric acid in the reaction mixture. Grzmil¹⁴ also proposed that the seed crystal pre-mixing stage, nucleation stage, and the formation stage of primary and secondary agglomerates should be carried out in separate kettles. However, it was difficult to achieve in practice because the nucleation and growth agglomeration of metatitanic acid were complementary, and there were no obvious boundaries in the hydrolysis process.

In this study, a microtubular reactor in the form of a spiral bend was used to conduct continuous hydrolysis experiments on titanyl sulfate. During the hydrolysis process, soluble titanium underwent phase transformation into solid metatitanic acid. The stability of fluid flow and transport of heat and mass in the tube are the key factors affecting the particle size and particle size distribution of the metatitanic acid produced.

Hayamizu¹⁵ and Yi and Liu¹⁶ performed the flow and heat transfer of water in a spiral bend pipe with an inner diameter of 20 mm, and it was found that the Dean vortex core of the secondary flow moved toward the elbow with the increase of the fluid Reynolds number at the inlet. When the curvature ratio of the spiral elbow was within 0.1–0.15 and the fluid Reynolds number was within 2280–6000, the heat transfer performance of the spiral elbow was the best.¹⁷ Chang et al.¹⁸ studied the uniform suspension flow and non-uniform suspension flow in the pipeline. It was found that a homogeneous suspension flow with an average particle size of 10 μm changed to a non-uniform suspension flow with increasing flow velocity.

Li et al.¹⁹ studied the influence of flow velocity on the hydrate particle size distribution and found that the particle size near the pipe wall was larger and the particle size in the center of the pipe was relatively small. The study on the aggregation of hydrate particles in the pipeline showed that the flow shear leads to the collision and aggregation of hydrate particles. Song et al.^{20–22} believed that with the increase of the hydrate volume fraction in the pipeline, the average size and maximum size of hydrate particles also increased accordingly. With the increase of the flow velocity in the tube, the maximum dimension of aggregates of the hydrate particles in the tube gradually decreased. The increase in the particle volume fraction results in increased friction, which is a key factor affecting the pressure drop of hydrate slurry flow.²³ Fluid flow can cause wear of the pipes. It has been pointed out²⁴ that maximum pressure appeared at the outer arch wall and the minimum pressure occurred in the inner arch wall. The impact of the hydrate slurry aggravates abrasion and corrosion at the outer arch wall of the elbow. At the same time, the pressure on the inner wall of the elbow dropped sharply, followed by cavitation and deformation of the pipeline. Therefore, although the increase in hydrate slurry flowrate helps to maintain a stable level of the maximum volume fraction of hydrate in the elbow, the operating conditions for industrial application should be chosen with comprehensive consideration of wear and tear caused by the pressure impact on the inner and outer walls of the elbow.

On the basis of literature analysis, by computational fluid dynamics (CFD) simulation and pre-experiments, a microtube with a cross-sectional size of φ 6 mm \times 1.5 mm was selected to construct a microchannel reactor. The reactor was innovatively

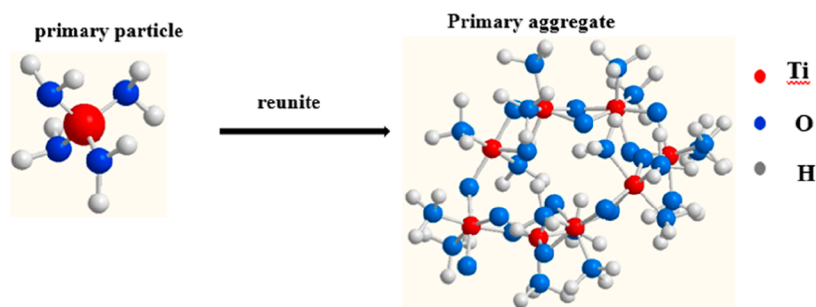


Figure 1. Agglomeration process during the hydrolysis of metatitanic acid.

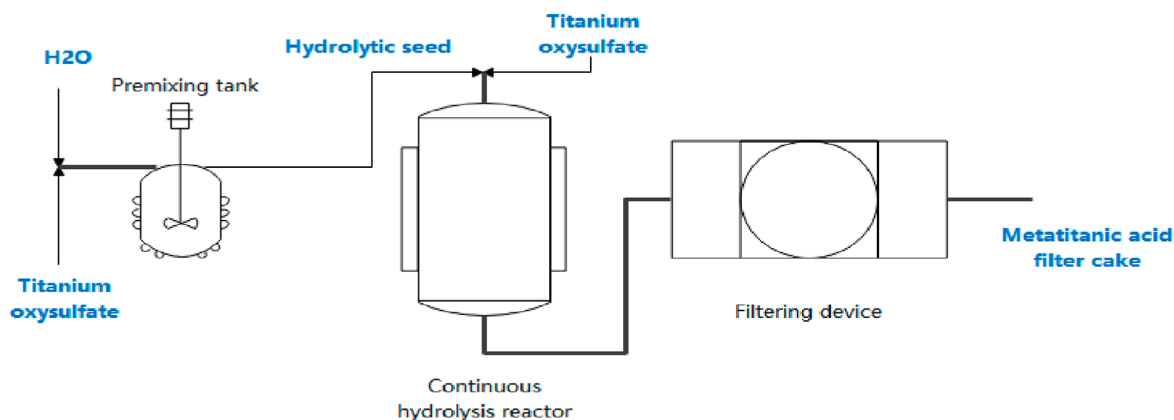


Figure 2. Schematic diagram of the continuous hydrolysis process.

applied in the study of continuous hydrolysis of titanyl sulfate. Taking the hydrolysis rate of the titanyl sulfate, particle size, and size distribution of metatitanic acid as reference indexes for evaluation, the volume ratio of the titanyl sulfate feed solution to the dilution water, the alkali concentration of the dilution water, and the flow rate of the feed were optimized by experiments. The continuous hydrolysis process of titanyl sulfate was developed. Compared with the batch hydrolysis process, the quality of metatitanic acid of the continuous process was greatly improved.

2. EXPERIMENTAL SECTION

2.1. Raw Material. The titanyl sulfate feed solution used in the experiment was provided by Lomon Baililian Co., Ltd., which was an acidolysis solution obtained by the reaction of ilmenite and sulfuric acid. The raw material indicators of the titanium solution are the total titanium concentration of 190 g/L, the iron-to-titanium mass ratio of 0.33, the F value of 1.95, and a concentration of 1.95 g/L Ti(III) (see Figure 1).

2.2. Experimental Methods. The authigenic seed crystals were used as the seed crystals of the hydrolysis reaction in experiments. By comparing the hydrolysis rate of continuous hydrolysis and batch hydrolysis and the particle size of metatitanic acid, the influence of key operating factors on the hydrolysis of titanyl sulfate was investigated. The schematic diagram of the continuous hydrolysis process is shown in Figure 2.

The experiments of continuous hydrolysis were conducted at 105 °C, while 0–1.2% NaOH solution was used as the dilution water, and the feed flow rate was 0.08–0.35 mL/s to keep the volume ratio of the dilution water to titanium solution ($V_{\text{water}}/V_{\text{TiOSO}_4}$) in the range of 1:2–1:4.5. The comparative experiments of continuous and batch hydrolysis of titanyl

sulfate were carried out, and the stability of continuous hydrolysis was investigated.

2.3. Testing and Analysis. The total titanium concentration, acidity value [$F = m_{\text{Effective acid}} (\text{g/L})/m_{\text{Total titanium}} (\text{g/L})$], Ti^{3+} concentration, and iron–titanium mass ratio [total iron content (g/L)/total titanium content (g/L)] were measured by chemical titration.²⁶

The calculation formula is the following: The hydrolysis rate of titanyl sulfate (R) is in reference to the ratio of the content of titanium and iron in the residual liquid obtained by filtering the metatitanic acid solid after the reaction to the content of titanium and iron in the reaction material titanyl sulfate solution.²⁶

$$R \% = \left(1 - \frac{\text{titanium in residual liquid (g)} / \text{Fe}^{2+} \text{ in residual liquid (g)}}{\text{Fe}^{2+} \text{ in titanyl sulfate solution (g)} / \text{titanium titanyl sulfate solution (g)}} \right) \times 100$$

%)

Particle size analysis of metatitanic acid. The hydrolyzed metatitanic acid was mixed with an appropriate amount of barium chloride solution to depolymerize the metatitanic acid secondary agglomerates into primary agglomerates. The NICOMP380 nanoparticle sizer analyzer of a particle sizing system was used to measure the particle size of the primary agglomerates. The particle size of metatitanic acid (secondary agglomerates) was determined using a Mastersizer 3000 laser particle sizer from Malvern Panalytical. The particle size distribution of metatitanic acid is expressed by crystal size distribution (CSD)

$$\text{CSD} = (D_{87}/D_{13})^{1/2}$$

An Optima 8000 plasma emission spectrometer of PerkinElmer was used to determine the elemental composition of metatitanic acid.

3. RESULTS AND DISCUSSION

3.1. Microchannel Reactor Design. The continuous flow reaction can be carried out in a microchannel reactor, where the reaction time can be precisely controlled by adjusting the flow rate of the reactants and the length of the microchannel. The microchannel reactor has great mass transfer and heat exchange efficiency due to its small tube diameter; its large heat exchange specific surface area greatly shortens the diffusion distance between reactants and enables fast supply and removal of heat. The above characteristics also grant the microchannel reactor a good inhibitory capacity on the burst reaction and improve the stability of the reaction process. Therefore, when the synthesis reaction is carried out in the microchannel reactor, there are few side reactions and the reaction conditions are easy to control. At the same time, the microchannel reactor also has the characteristics of no scale-up effect, high process development efficiency, and low R&D cost, making the microchannel reactor a popular tool in the development of the continuous process.

In this work, the flow inside the $\phi 6 \text{ mm} \times 1.5 \text{ mm}$ pipeline of 1 km length was simulated and analyzed with CFD simulation, while the $k-\varepsilon$ model was adopted as the turbulent model. During the calculation, we set the medium to be water, the particle size of solid suspended particles to be $4 \mu\text{m}$, and the rest of the parameters to be default values. The velocity nephograms of the rectangular pipeline and the folded pipeline are shown in Figure 3a,b. It has been established by simulation that the volume fraction distribution of the solid phase is relatively uniform, and there is no blocking by the solid phase. The power loss increased gradually with the length of the pipeline. As shown in Figure 3c,d, there was a velocity difference between the inner and outer radii on the bending section, and the flow velocity was higher at the inner bend. There was power loss and greater wear close to the near inner wall of the tube. The bending form of the pipeline as shown in Figure 3e was selected in general consideration of pipeline resistance, elbow abrasion, and efficiency for space utilization. In order to overcome the flow resistance, the microreactor was constructed in the form of segmental supplementary conveying power. The microtube assembly was placed in a heated water bath device to form a continuous hydrolysis reactor for metatitanic acid.

3.2. Effect of the Volume Ratio of Dilution Water to Titanium Liquid on the Continuous Hydrolysis Process.

Titanium liquid and pure water are mixed prior to hydrolysis, and the volume ratio of the two liquids directly affects the initial concentration of the titanium liquid in the hydrolysis reaction and the number of crystal seeds generated by the reaction. Batch and continuous hydrolysis experiments were carried out with the volume ratios of dilution water and titanium liquid of 1:2, 1:3, 1:3.5, 1:4, and 1:4.5. The reaction temperature was kept at $105 \text{ }^\circ\text{C}$ to avoid the phenomenon of slurry boiling during the hydrolysis process.²⁵ The material flow rate of the continuous hydrolysis reaction was 0.35 mL/s . The experiments were repeated four times for each condition, and the hydrolysis rate was the average value of the four experiments. Taking the average value reduces the influence of

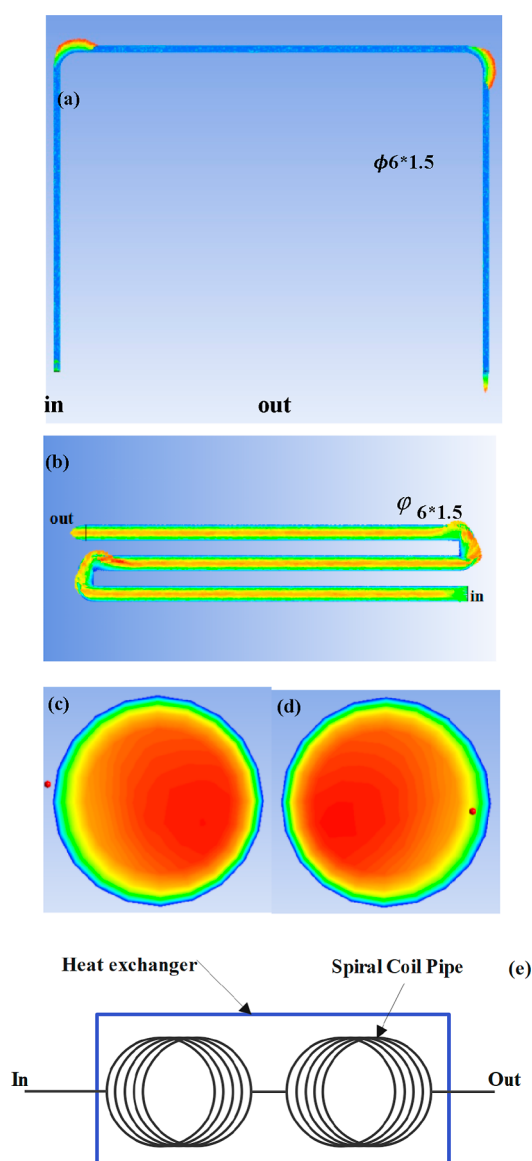


Figure 3. Velocity nephograms of two pipeline layout modes, respectively, (a) rectangular pipeline and (b) folded pipeline. (c,d) Concentration distribution diagram of the bending part of the pipeline. (e) Schematic diagram of the pipeline layout.

deviation on the experimental results. The profile of the hydrolysis rate of titanyl sulfate under different experimental conditions is shown in Figure 4.

According to the experimental data, under the same volume ratio of dilution water to titanium liquid ($V_{\text{water}}/V_{\text{TiOSO}_4}$), a hydrolysis rate of 90% can be achieved earlier in the continuous hydrolysis compared to the batch operation. Hydrolysis of titanyl sulfate is an endothermic reaction. The continuous hydrolysis using a microtubular reactor has a better heat transfer effect and less continuous reaction back-mixing, which exhibits better performance in mass and heat transfer as compared to that of batch tank reactors. Regardless of whether it was a batch hydrolysis method or a continuous hydrolysis method, the more the amount of dilution water added, the shorter the time required to achieve a 90% hydrolysis rate and the higher the final hydrolysis rate. This was explained by the fact that the more the amount of dilution water, the lower the concentration of sulfuric acid in the reaction system, which

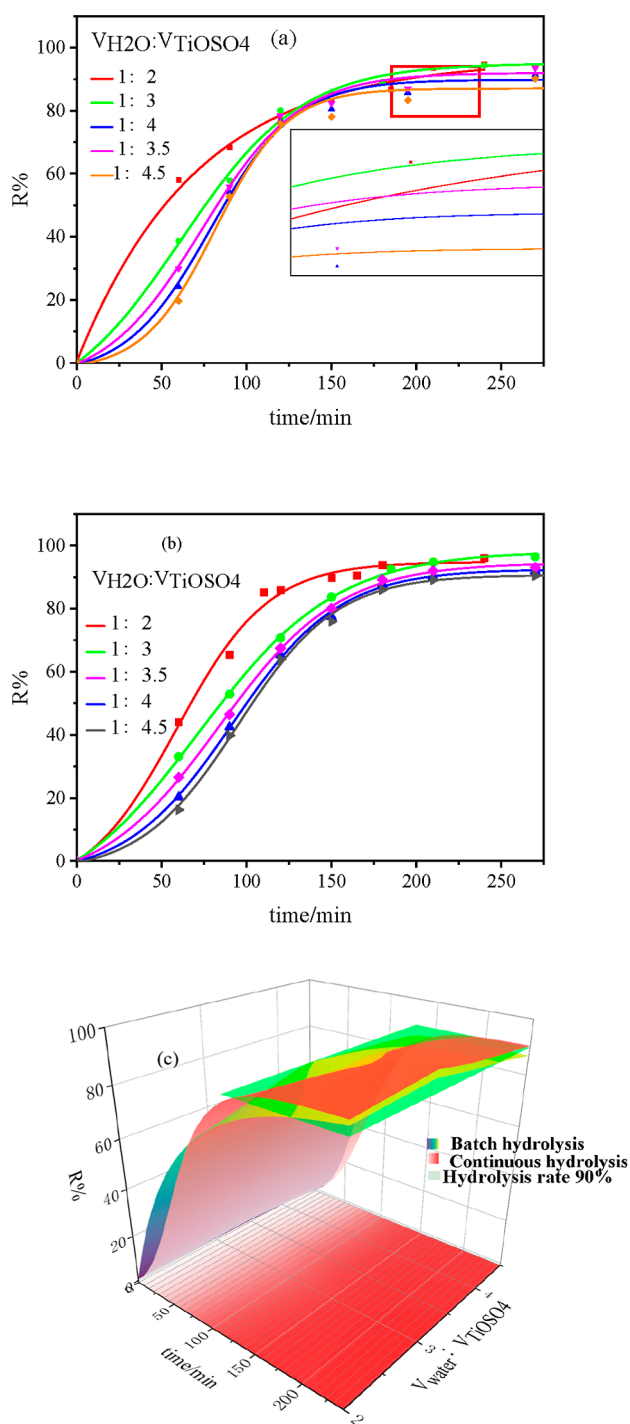


Figure 4. Comparison of the hydrolysis rates between batch hydrolysis and continuous hydrolysis under different $V_{\text{water}}/V_{\text{TiOSO}_4}$: (a) batch hydrolysis rate, (b) continuous hydrolysis rate, and (c) variation of the hydrolysis rate with the reaction time under different $V_{\text{water}}/V_{\text{TiOSO}_4}$.

would promote hydrolysis. However, too much dilution water also reduced the concentration of titanyl sulfate, which weakened the growth power of metatitanic acid crystals and reduced the total hydrolysis rate of the reaction. This can be seen from the difference between the hydrolysis rate curve of batch hydrolysis under $V_{\text{water}}/V_{\text{TiOSO}_4} = 1:2$ and other curves.⁹ When $V_{\text{water}}/V_{\text{TiOSO}_4} = 1:3$, the highest hydrolysis rate of 96%

was reached after 4 h of hydrolysis. The deviation of the hydrolysis rate of the four repeated experiments under each condition was analyzed, finding that the maximum deviation of continuous hydrolysis was ($\pm 0.25\%$), and the maximum deviation of batch hydrolysis was ($\pm 0.41\%$). The experimental data prove that the stability of continuous hydrolysis is better than that of batch hydrolysis.

The study on the nucleation and agglomeration mechanism of metatitanic acid obtained from the hydrolysis reaction of titanyl sulfate shows that the primary agglomerated particle size was an important factor in determining the secondary agglomerated particle size of metatitanic acid and the particle size of rutile TiO_2 in subsequent calcination.^{12,26} The morphology and particle size of rutile TiO_2 products affected pigment properties such as hiding power, achromatic power, and fluidity. The primary agglomeration particle size of metatitanic acid obtained from batch and continuous operation were measured, and the results are shown in Figure 5 and Table 1.

When the range of $V_{\text{water}}/V_{\text{TiOSO}_4}$ was between 1:2 and 1:4.5, the particle size D_{50} of agglomerates obtained by batch hydrolysis was 44.50–62.81 nm, CSD was 1.773–1.628, while the particle size D_{50} of primary agglomerates obtained by continuous hydrolysis was 39.66–54.10 nm and CSD was from 1.703 to 1.538. The size of primary agglomerate particles prepared by continuous hydrolysis was smaller than that of batch hydrolysis, and the distribution was more uniform because microtubular reactors were flat plug flow reactors with low back-mixing and high heat transfer efficiency, in which explosive nucleation and early rapid hydrolysis were avoided. The hydrolysis reaction proceeded in an orderly manner along the length of the reaction tube. The obtained metatitanic acid particles were uniform in size, and the hydrolysis rate was slightly higher than that of the batch hydrolysis process.

3.3. Influence of Alkali Concentration of the Dilution Water on the Continuous Hydrolysis Process. The variation of the hydrolysis rate and the primary agglomeration particle size of continuous hydrolysis and batch hydrolysis with the alkali (NaOH) concentration of dilution water of 0, 0.4, 0.8, and 1.2%, respectively, was experimentally investigated. The reaction temperature of the experiment was 105 °C, $V_{\text{water}}/V_{\text{TiOSO}_4}$ was 1:3, and the continuous hydrolysis flow rate was 0.35 mL/s. The experiments were repeated four times for each condition, and the average value of the four experiments was taken for the hydrolysis rate to reduce the influence of deviation on the experimental results. The results are shown in Figure 6.

Increasing the alkali (NaOH) concentration of the dilution water will reduce the acidity of the titanium solution and promote the progress of hydrolysis. The experimental results showed that the hydrolysis rate of continuous hydrolysis was greater than that of batch hydrolysis when the NaOH mass concentration was of 0–0.8%, and the difference in the hydrolysis rate became smaller when the NaOH mass concentration was 0.8–1.2%. The total hydrolysis rate of continuous hydrolysis was higher than that of batch hydrolysis under the same alkali concentration. Analyzing the deviation of the hydrolysis rate of the four repeated experiments under each condition, the maximum deviation of the hydrolysis rate of continuous hydrolysis is ($\pm 0.28\%$), and the maximum deviation of the hydrolysis rate of intermittent hydrolysis is ($\pm 0.46\%$).

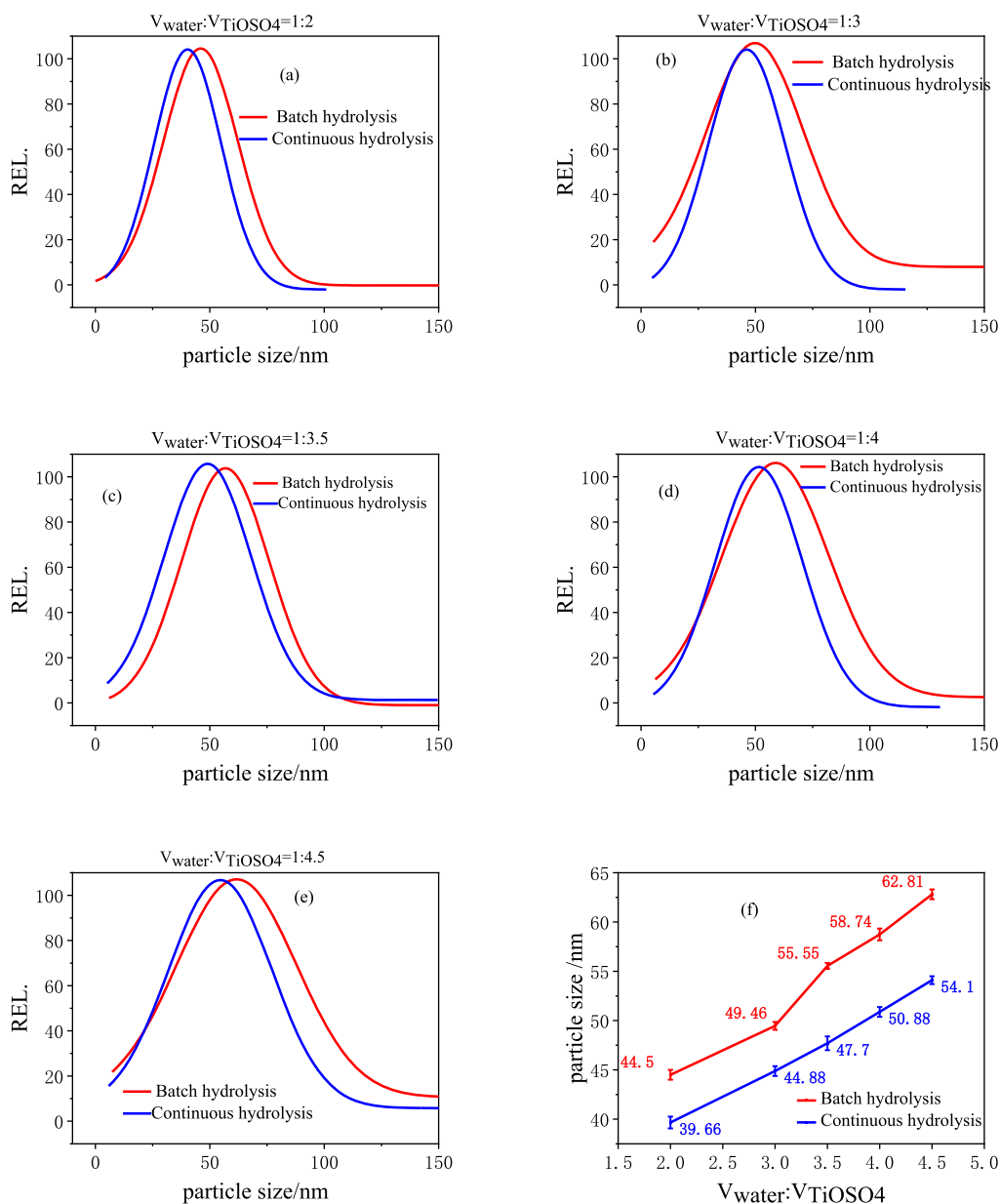


Figure 5. Comparison of the primary agglomerate particle size distribution of continuous hydrolysis and intermittent hydrolysis under different $V_{\text{water}}/V_{\text{TiOSO}_4}$ (a–e) particle size distribution, and (f) primary aggregate size.

As the alkali (NaOH) concentration of the dilution water increased, the particle size D50 of primary agglomerates of batch hydrolysis decreased from 49.14 to 41.66 nm and then increased to 55.55 nm, and the CSD increased from 1.661 to 1.756. For continuous hydrolysis, the particle size D50 of primary agglomerates decreased from 44.82 to 40.60 nm and then increased to 48.76 nm, and the particle size distribution became narrow first and then the edge became wider, and the corresponding CSD increased from 1.601 to 1.662. Decreased acidity of the titanium solution can promote the formation of crystal nuclei and facilitate the progress of hydrolysis. Meanwhile, an excessively high dilution water alkali concentration will affect the stability of the hydrolysis seed crystal and will cause partial premature hydrolysis, which broadens the particle size distribution of the hydrolysate metatitanic acid. Comparing continuous hydrolysis and batch hydrolysis, it was found that the variations of the particle size and the size

distribution of the primary agglomeration of continuous hydrolysis were 40.6–48.76 nm and 1.601 to 1.662, which were smaller than those of batch operation (Figure 7, Table 2).

3.4. Influence of the Flow Velocity on the Continuous Hydrolysis Process. The flow rates of 0.08, 0.15, 0.23, 0.26, and 0.35 mL/s were used for continuous hydrolysis, while the reaction temperature was 105 °C and $V_{\text{water}}/V_{\text{TiOSO}_4} = 1:3$. The hydrolysis rates of the reaction solution at different reaction times were analyzed, and the result is shown in Figure 8.

According to the hydrolysis rate change curve, it is obvious that an increase in the flow rate increases the hydrolysis rate in the early stage of hydrolysis, and the hydrolysis rate of the total hydrolysis reaction increases. The increase in flow velocity increases the dispersion capacity, which is conducive to heat exchange and mass transfer. The particle size growth is positively related to the flow velocity, which promotes the nucleation in the early stage of the hydrolysis reaction and the

Table 1. Effect of $V_{\text{water}}/V_{\text{TiOSO}_4}$ on Particle Size and Particle Size Distribution of Metatitanic Acid Obtained by Different Hydrolysis Methods

$V_{\text{water}}/V_{\text{TiOSO}_4}$	primary aggregate size/nm	CSD	secondary agglomerations/ μm
Continuous Hydrolysis			
1:2	39.66	1.703	4.33
1:3	44.88	1.601	3.69
1:3.5	47.70	1.574	3.22
1:4	50.88	1.553	3.08
1:4.5	54.10	1.538	2.67
Batch Hydrolysis			
1:2	44.50	1.773	3.72
1:3	49.45	1.667	3.43
1:3.5	55.55	1.643	2.68
1:4	58.74	1.617	2.48
1:4.5	62.81	1.628	2.03

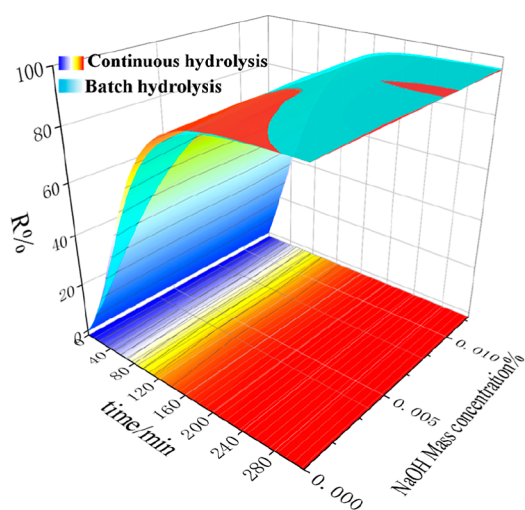


Figure 6. Variation of the hydrolysis rate with the reaction time under different alkali (NaOH) concentrations of dilution water.

crystal growth in the later stage. The particle size of the primary agglomerate of the metatitanic acid depolymerization product after hydrolysis has been investigated, as shown in Figure 9 and Table 3.

The experiment results indicated that as the flow rate increased from 0.08 to 0.35 mL/s, the particle size D50 of the primary agglomeration decreased from 59.30 to 43.11 nm, and CSD became narrow from 1.854 to 1.502. The slower the flow rate was, the weaker the capacity of fluid carried the particles in the slurry, which was more conducive to the growth of primary crystals of metatitanic acid. Hence, the particle size of primary agglomerates formed by the agglomeration of primary metatitanic acid crystals was smaller. The reduction of the primary agglomerate particle size was favorable for the formation of big-size metatitanic acid (secondary agglomerations). Therefore, within the flow rate range of the experiment, the particle size of the hydrolyzed product metatitanic acid was proportional to the flow rate, increasing with the increase of flow rate.

3.5. Stability Investigation of the Continuous Hydrolysis Process. In summary, the optimal operating conditions for continuous hydrolysis were obtained by the study as follows: $V_{\text{water}}/V_{\text{TiOSO}_4}$ was 1:3, the flow rate was 0.26

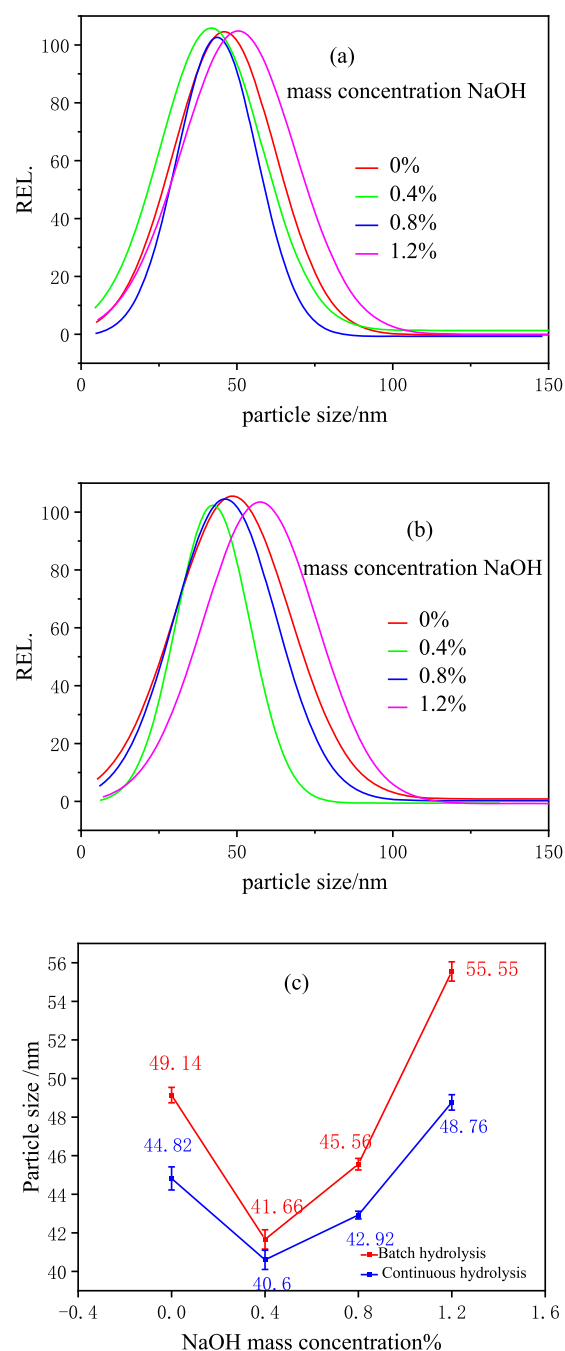


Figure 7. Comparison of the primary agglomerate particle size and size distribution of continuous hydrolysis and batch hydrolysis under different alkali (NaOH) concentrations of dilution water. (a) Continuous hydrolysis, (b) batch hydrolysis, and (c) comparison between the two processes.

mL/s, and the reaction time was more than 210 min. Under the optimized conditions, the hydrolysis rate was more than 94%, and the average particle size of primary agglomeration was 48 nm. Compared with the batch tank hydrolysis, the reaction time was shortened by more than 40 min, and the particle size of the primary agglomeration was 8 nm smaller.

Using the same experimental device, a 150 h duration of continuous hydrolysis experiment was carried out according to the above optimal reaction conditions, and samples were taken at the outlet of the equipment at certain time intervals. The hydrolysis rate and the primary agglomeration particle size of

Table 2. Effect of Alkali (NaOH) Concentration of Dilution Water on Particle Size and Particle Size Distribution of Metatitanic Acid Obtained by Different Hydrolysis Methods

NaOH mass concentrations %	primary aggregate size/nm	CSD	secondary agglomerations/ μm
Continuous Hydrolysis			
0	44.82	1.601	3.69
0.4	40.60	1.628	4.33
0.8	42.92	1.643	3.49
1.2	48.76	1.662	3.08
Batch Hydrolysis			
0	49.14	1.661	2.68
0.4	41.66	1.692	2.81
0.8	45.56	1.723	2.35
1.2	55.56	1.756	2.03

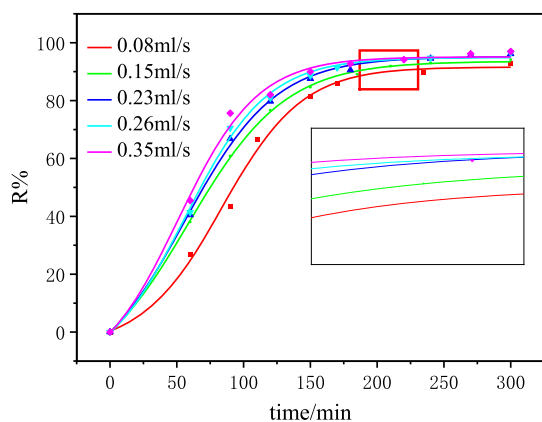


Figure 8. Relationship between the hydrolysis rate and the reaction time of continuous hydrolysis at different flow velocities.

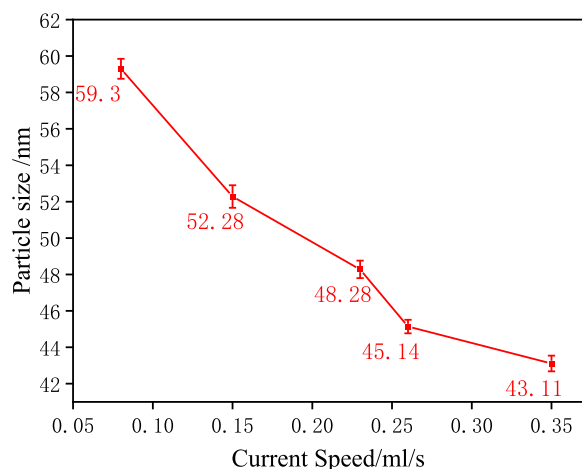


Figure 9. Particle size of primary agglomerates in continuous hydrolysis at different flow rates.

samples of metatitanic acid were measured, and the data obtained are as follows:

According to the experimental data, the average hydrolysis rate of titanium sulfate was 95.32%, and the fluctuation range was [(-0.201%)-(+0.152%)], the average particle size of primary agglomeration was 45.43 nm, and the fluctuation range was [(-0.661%)-(+0.733%)], the average CSD was 1.702, and the fluctuation range was ((-1.624%)-(+1.971%)). The continuous hydrolysis experimental oper-

Table 3. Primary Agglomerate Particle Size and CSD of Continuous Hydrolysate at Different Flow Rates

flow rate mL/s	primary aggregate size/nm	CSD	secondary agglomerations/ μm
0.08	59.30	1.854	2.57
0.15	52.28	1.791	2.72
0.23	48.28	1.732	3.15
0.26	45.14	1.633	3.58
0.35	43.11	1.502	4.31

ation exhibited robust stability, and no blockage was found in the microtube (Table 4).

Table 4. Indexes of Export Products for Long-Term Continuous Hydrolysis

time/h	R/%	primary agglomeration particles size/nm	CSD
7	95.43	45.21	1.633
35	95.31	45.76	1.611
50	95.13	45.27	1.618
71	95.24	45.39	1.647
95	95.35	45.13	1.671
118	95.47	45.72	1.639
141	95.33	45.53	1.651

4. CONCLUSIONS

The study results show that the continuous hydrolysis operation using a microtubular reactor is more concise and efficient than the batch kettle hydrolysis operation. The former can obtain a higher hydrolysis rate of titanyl sulfate and smaller primary agglomeration particle size of metatitanic acid.

For the continuous hydrolysis reaction process, the increase of the flow rate promotes mass transfer and heat transfer, which is conducive to the progress of hydrolysis reaction, thereby increasing the hydrolysis rate of titanyl sulfate. At the same time, the ability to carry particles of fluid becomes stronger, which promotes the nucleation of metatitanic acid and is beneficial to form primary agglomerates of metatitanic acid with a larger particle size. The increase of the alkali concentration of the dilution water enhances the nucleation of metatitanic acid and the hydrolysis reaction. However, an excessive alkali concentration of the dilution water will lead to explosive nucleation, thus increasing the primary agglomeration particle size of metatitanic acid.

It is experimentally determined that the optimal conditions for continuous hydrolysis is operation at flow rate of 0.26 mL/s and a $V_{\text{water}}/V_{\text{TiOSO}_4}$ ratio of 1:3 within 210 min. Under the conditions, the hydrolysis rate can reach more than 94%, and the particle size D50 of the primary agglomeration is 48 nm. The results of a 150 h duration continuous hydrolysis experiment showed that the fluctuations of the hydrolysis rate, primary agglomeration particle size, and particle size distribution were small. The continuous hydrolysis experimental operation exhibited robust stability, and no blockage was found in the microtube.

The development of the continuous process of titanium dioxide using a sulfuric acid method can have a certain impact on the production of titanium dioxide with special properties.

AUTHOR INFORMATION

Corresponding Authors

Kui Chen – State Key Laboratory of Chemical Engineering, School of Chemical Engineering, East China University of Science and Technology, Shanghai 200237, P.R. China; orcid.org/0000-0003-2384-0347; Email: chenkui@ecust.edu.cn

Yu Rong Zhang – Lomon Billions Group Co., Ltd., Jiaozuo, Henan 454191, China; Email: zyr@lomon.com

Authors

Wenbo Chang – State Key Laboratory of Chemical Engineering, School of Chemical Engineering, East China University of Science and Technology, Shanghai 200237, P.R. China

Jianli Chen – Lomon Billions Group Co., Ltd., Jiaozuo, Henan 454191, China

Jun Dou – Lomon Billions Group Co., Ltd., Jiaozuo, Henan 454191, China

Bin Wu – State Key Laboratory of Chemical Engineering, School of Chemical Engineering, East China University of Science and Technology, Shanghai 200237, P.R. China

Complete contact information is available at:
<https://pubs.acs.org/10.1021/acsomega.2c01621>

Notes

The authors declare no competing financial interest.

REFERENCES

- (1) Chen, W. J.; Xu, W. J.; Dai, J. J. Research on the optimization of titanium dioxide hydrolysis process[J]. *Shandong Chem. Ind.* **2012**, *41*, 1119–1213.
- (2) Sun, Z.; Zheng, L.; Zheng, S.; Frost, R. L. Preparation and characterization of TiO₂/acid leached serpentinite tailings composites and their photocatalytic reduction of Chromium(VI)[J]. *J. Colloid Interface Sci.* **2013**, *404*, 102–109.
- (3) Shen, X. X. Development status and product performance comparison of domestic and foreign titanium dioxide varieties. *Metall. Series* **2012**, *5*, 46–50.
- (4) Pal, M.; Wan, L.; Zhu, Y.; et al. Scalable synthesis of mesoporous titania microspheres via spray-drying method. *J. Colloid Interface Sci.* **2016**, *479*, 150–159.
- (5) Qin, Y. *Study on Organic Modification of Titanium Dioxide and Hydrolysis of Titanyl Sulfate [D]*; Wuhan University of Science and Technology: Hubei, 2013.
- (6) Hixson, A. W.; Fredrickson, R. E. C. Hydrolysis of Titanyl Sulfate Solutions. *Ind. Eng. Chem.* **1945**, *37*, 678–684.
- (7) Santacesatia, E.; Tonello, M.; Storti, G.; Pace, R. C.; Carra, S. Kinetics of titanium dioxide precipitation by thermal hydrolysis[J]. *J. Colloid Interface Sci.* **1986**, *111*, 45–53.
- (8) Tian, C. X.; Du, J. Q.; Chen, X. H.; Ma, W. P.; Luo, Z. Q.; Cheng, X. Z.; Hu, H. F.; Liu, D. J. Influence of hydrolysis in sulfate process on titania pigment producing[J]. *Trans. Nonferrous Metals Soc. China* **2009**, *19*, 829–833.
- (9) Yu, X. M.; Liu, D. J.; Xiao, Y. H.; Xu, C. H.; Chao, L. Z. Study on the hydrolysis parameters of titanium dioxide from blast furnace slag containing titanium[J]. *Inorg. Salt Ind.* **2008**, *01*, 42–44.
- (10) Yang, L.; Yi, D. L.; Wang, C.; Wu, L. Stability analysis of titanium sulfate solution and particle size control of metatitanic acid[J]. *Inorg. Salt Ind.* **2015**, *04*, 26–29.
- (11) Sathyamoorthy, S.; Moggridge, G. D.; Hounslow, M. J. Particle Formation during Anatase Precipitation of Seeded Titanyl Sulfate Solution. *Cryst. Growth Des.* **2001**, *1*, 123–129.
- (12) Zhu, R. M.; Chen, K.; Zhu, J. W.; Zhou, X. K.; Lin, F. R. The effect of seed crystal on the hydrolysis process and brightness of titanium dioxide[J]. *Inorg. Salt Ind.* **2019**, *51*, 30–34.
- (13) Grzmil, B.; Grela, D.; Kic, B. Effects of processing parameters on hydrolysis of TiOSO₄. *Pol. J. Chem. Technol.* **2009**, *11*, 15–21.
- (14) Grzmil, B.; Grela, D.; Kic, B. Formation of hydrated titanium dioxide from seeded titanil sulphate solution. *Chem. Pap.* **2009**, *63*, 217–225.
- (15) Datta, A. K.; Hayamizu, Y.; Kouchi, T.; Nagata, Y.; Yamamoto, K.; Yanase, S. Numerical Study of Turbulent Helical Pipe Flow With Comparison to the Experimental Results. *J. Fluids Eng.* **2017**, *139*, 091204–109120413.
- (16) Yi, J.; Liu, Z.-H.; Wang, J. Heat transfer characteristics of the evaporator section using small helical coiled pipes in a looped heat pipe[J]. *Appl. Therm. Eng.* **2003**, *23*, 89–99.
- (17) Feng, L. L.; Xu, R. S.; Feng, J. Y. Numerical simulation of flow and heat transfer characteristics in spiral bend pipe[J]. *J. Drain. Irrig. Mach. Eng.* **2020**, *38*, 697–701.
- (18) Chang, K.; Rao, Y. C.; Wang, S. H. L. Numerical simulation of spiral flow of hydrate particles in gas pipeline[J]. *Petrol. Mach.* **2017**, *45*, 107–113.
- (19) Li, L. J.; Zhao, S. H.; Ding, B. Y.; Rao, Y. C.; Wang, S. L. Numerical simulation of spiral flow characteristics of natural gas hydrate particles in elbows[J]. *Nat. Gas. Chem. Ind.* **2021**, *46*, 81–86.
- (20) Song, G. C.; Li, Y. X.; Wang, W. C.; Jiang, K.; Shi, Z. Z.; Yao, S. P. Hydrate aggregation kinetic model based on population equilibrium theory[J]. *Hwahak Kwa Kongop Ui Chinbo* **2018**, *37*, 80–87.
- (21) Song, G. C.; Li, Y. X.; Wang, W. C.; Yao, S. P.; Wei, D.; Yan, B. Numerical simulation of hydrate deposition characteristics in pipes based on group balance theory. *Petrochem. Ind.* **2018**, *47*, 153–163.
- (22) Balakin, B. V.; Lo, S.; Kosinski, P.; Hoffmann, A. C. Modelling agglomeration and deposition of gas hydrates in industrial pipelines with combined CFD-PBM technique[J]. *Chem. Eng. Sci.* **2016**, *153*, 45–57.
- (23) Zhong, Y. H.; Qing, Y. L.; Yang, H. C.; Li, L. L.; Liu, T.; Jiang, P. Numerical simulation of flow characteristics of hydrate slurry in pipeline based on Fluent[J]. *Nat. Gas. Chem. Ind.* **2021**, *46*, 126–132.
- (24) Sun, X.; Wang, L.; Ren, Z. Q. Safety analysis of hydrate slurry flow in horizontal elbows[J]. *Chem. Eng.* **2018**, *46*, 45–50.
- (25) Anhui JX Titanium Bai (Group) Co. Ltd. A method for measuring the hydrolysis rate of titanium dioxide produced by sulfuric acid method. CN 202010057270.1 A, 2020.
- (26) Chen, K.; Yan, X. H.; Wu, P. S.; Wang, Z. N.; Wu, B.; Lin, F. R. Effect of sulfate on crystal phase transition and crystal growth of titanium dioxide in metatitanic acid calcination. *Phase Transitions* **2021**, *94*, 353.